The Open Biomedical Engineering Journal
DOI: 10.2174/0118741207500118260731073145, 2026, 20, e18741207500118
ISSN: 1874-1207
1

RESEARCH ARTICLE **OPEN ACCESS**

Nano-Encapsulated Curcumin Improves Ovarian and Uterine Recovery from Cadmium Toxicity in Rats

Mohammed N. A. Al-Muhja[1] and Jabbar A. A. Al-Saaidi[2,*]

[1]*Department of Physiology, Pharmacology, and Biochemistry, College of Veterinary Medicine, University of Al-Qadisiyah, Al Diwaneyah, Iraq*
[2]*Department of Basic Sciences, College of Dentistry, Al-Ayen Iraqi University, Nasiriya, Iraq*

Abstract:

Introduction/Objectives: Cadmium (Cd) is a ubiquitous environmental toxicant that causes adverse effects on female reproductive organs. Curcumin (Cm) has potent antioxidant and anti-inflammatory properties, but it has low solubility and bioavailability. The present study aimed to evaluate and compare the protective effects of native Cm and polycaprolactone/polyvinyl alcohol-based curcumin nanoparticles (PCL/PVA/Cm NPs) against Cd-induced ovarian and uterine toxicity in female rats through histopathological, semi-quantitative, and morphometric analyses.

Methods: Forty-eight adult female rats were randomly assigned to six groups (n = 8/group): control, Cd, Cm, Cd + Cm, PCL/PVA/Cm NPs, and Cd + PCL/PVA/Cm NPs. Treatments were given orally for four weeks. Ovarian and uterine tissues were collected at the end of the experimental period for histopathological analysis, semi-quantitative histological scoring, and morphometric evaluation.

Results: Cd exposure induced marked ovarian and uterine histopathological changes, including follicular atresia, degeneration of corpora lutea, vascular congestion, thinning of the endometrial epithelium, glandular atrophy and inflammatory cell infiltration, and reduced endometrial and myometrial thickness. Interestingly, treatment with free Cm maintained normal granulosa cell proliferation and uterine morphology. Administration of Cm along with Cd revealed partial histological recovery compared with the group treated with Cd alone. On the other hand, PCL/PVA-encapsulated Cm showed the most significant histological improvements with signs of active folliculogenesis and normal uterine structure. Interestingly, the group treated with Cd + PCL/PVA/Cm NPs showed almost complete recovery of ovarian and uterine structure with histological scores comparable to those of the control groups.

Discussion: The significant restoration of ovarian and uterine tissues and folliculogenesis in PCL/PVA/Cm NPs-treated animals could be attributed to the enhanced bioavailability and sustained release of Cm.

Conclusion: PCL/PVA/Cm NPs exhibited greater protective and restorative effects against Cd-induced reproductive toxicity than native Cm, indicating that nanoparticle-mediated delivery of curcumin may represent an effective strategy for protecting the female reproductive system against heavy metal-induced damage.

Keywords: Cadmium toxicity, Curcumin nanoparticles, Polycaprolactone, Polyvinyl Alcohol, Female reproductive toxicity, Uterine morphology, Ovarian histopathology, Nanomedicine.

*Address correspondence to this author at the Department of Basic Sciences, College of Dentistry, Al-Ayen Iraqi University, Nasiriya, Iraq; Tel: +9647731901075; E-mail: jabbar.alsaaidi@alayen.edu.iq

Cite as: Al-Muhja M, Al-Saaidi J. Nano-Encapsulated Curcumin Improves Ovarian and Uterine Recovery from Cadmium Toxicity in Rats. Open Biomed Eng J, 2026; 20: e18741207500118.
http://dx.doi.org/10.2174/0118741207500118260731073145

Received: April 01, 2026
Revised: June 01, 2026
Accepted: June 04, 2026
Published: August 05, 2026

1. INTRODUCTION

Cadmium (Cd) is widely used in industry for corrosion-resistant coatings, rechargeable batteries, metal alloys, nuclear reactor control rods, and stable pigments in high-grade paints because of its durability, lightweight properties, neutron absorption capacity, and resistance to oxidation [1].

Cd is a common environmental heavy metal found in the surroundings, with high toxicity, persistence, and bioaccumulation, which poses a significant threat to human and animal health. By contrast, it is regularly released into the environment through industrial emissions of toxic gases, cigarette smoke, contaminated food and water supplies, with resulting long-term exposure in many populations. Cd is classified as a non-essential metal, and no physiological role has been identified for Cd in biological systems despite its ability to accumulate readily into tissues and interfere with normal cellular activities. One of the organs most sensitive to Cd toxicity is the reproductive system, and in particular, the female reproductive organs [2, 3].

The female reproductive system is extremely responsive to toxic environmental pollutants because of its intricate hormonal control and the sensitive mechanisms of folliculogenesis, ovulation, and steroidogenesis. It is well established that Cd exposure affects reproductive performance by mechanisms of oxidative stress, inflammation, apoptosis, and disruption of the hypothalamic–pituitary–gonadal axis [4, 5]. Overproduction of Reactive Oxygen Species (ROS), which results in oxidative injury of the lipid, protein, and nucleic acid biomolecules, is one of the major mechanisms underlying Cd-mediated toxicity. Concomitantly, Cd inhibits intrinsic antioxidant defense systems, which further aggravates cellular damage in reproductive tissues [6, 7].

Both experimental and epidemiological investigations indicate that Cd action induces structural and functional changes in female reproductive organs. These changes include degeneration of ovarian follicles, damage to uterine tissues, hormonal imbalance, and lowered fertility potential [8, 9]. Cd has also been found to interfere with reproductive hormone secretion, including Follicle-Stimulating Hormone (FSH), Luteinizing Hormone (LH), and estrogen, resulting in damage to ovarian function and reproductive cycles [10]. Cd also exhibits estrogen mimetic activity and functions as an endocrine disruptor, which can alter regular reproductive signaling pathways [11]. Due to these harmful effects, the identification of protective agents that can alleviate Cd-induced reproductive toxicity has become a significant area of interest in biomedical research.

Natural antioxidants have been widely studied as possible therapeutic agents to combat metallotoxicity. Curcumin (Cm), the main medicinal polyphenolic compound from *Curcuma longa*, is one of these compounds that have been reported for their various pharmacological effects. Cm has strong antioxidant, anti-inflammatory, anti-apoptotic, and metal-chelating properties with the potential to protect biological systems from oxidative destruction [12, 13]. In the reproductive system, Cm was reported to ameliorate ovarian function, regulate reproductive hormones, and modulate oxidative and inflammatory damage in ovarian tissues [14, 15].

Various experimental studies illustrate that Cm has a protective role against reproductive toxicity. Cm is known to increase the activity of antioxidant enzymes, decrease lipid peroxidation, and regulate signaling pathways relating to oxidative stress and apoptosis. Furthermore, Cm has been demonstrated to protect against follicular damage and improve endocrine or reproductive performance of ovarian tissue under toxic or stressful conditions [16, 17]. Moreover, Cm may modulate important cellular signaling pathways like Nuclear factor erythroid 2-related factor (Nrf2/HO-1) and Phosphoinositide 3-Kinase/ Protein Kinase B (PI3K/Akt) that are vital for cellular defense systems and tissue protection [18, 19].

Although native Cm has demonstrated some promising biological effects, its clinical use as a drug is hampered by serious pharmacokinetic disadvantages such as poor solubility in water and rapid metabolism, low bioavailability, and limited tissue distribution [20, 21]. These restrictions greatly limit the efficacy of Cm when taken in its most classical type. In order to overcome these challenges, recent advances in nanotechnology have been directed toward Cm-based nano-formulations that improve stability, bioavailability, and targeted delivery [22, 23].

Owing to this, Cm nanoparticles exhibited superior pharmacological activity over free Cm owing to increased cellular uptake and a prolonged release profile [24, 25] found that nano-Cm formulations manifested more potent antioxidant and anti-inflammatory properties, as well as higher therapeutic efficacy, in experimental models of toxicity than traditional Cm preparations [26, 27]. Nano-Cm protects ovarian cells from oxidative damage, enhances follicular development, and restores hormonal balance in reproductive tissues undergoing stressed conditions [28, 29]. These findings collectively underscore the potential of Cm nanoparticles as an innovative therapeutic approach for countering reproductive toxicity.

Many studies have already been conducted on Cd-induced toxicity as well as the protective efficacy of Cm; however, there is still a scarcity of comparative studies testing the application of native Cm *versus* nano-formulated Cm in female reproductive toxicity. Most available research into Cm has studied general antioxidant effects or male reproductive systems specifically, which leaves a gap in understanding how Cm or Cm nanoparticles protect female reproductive tissues against Cd toxicity. This gap needs to be addressed for the development of better therapeutic strategies that enhance the biological efficiency of Cm-based interventions.

Accordingly, the current study aimed to comparatively assess the protective effects of native Cm and Cm nanoparticles on Cd-induced reproductive organ toxicity. Through the assessment of histopathological changes, this

study attempts to elucidate whether nano-formulated Cm offers greater protection for female reproductive tissues compared to native Cm. This study is expected to make a significant contribution to the field of nanomedicine, which would generate scientific evidence for evolving therapeutic strategies to safeguard reproductive health against environmental toxicants.

2. MATERIALS AND METHODS

2.1. Animal Models and Ethical Considerations

This study was conducted from October 2024 to April 2025 at the animal house in the College of Veterinary Medicine, University of Al-Qadisiyah, Iraq. Adult Wistar female rats (provided by the animal house of the same College) were used for the ovarian and uterine toxicology study due to their extensive characterization in both reproductive and toxicological studies. The animals were kept under controlled environmental conditions (temperature, 23 ± 2°C; relative humidity, ~50–60%) in polypropylene cages. Rats were kept in a temperature- and humidity-controlled room (standard 12 h light/12 h dark cycle; lights on: 06:00 a.m., off: 06:00 p.m.).

Experimental animals were given a standardized laboratory pellet diet (crude protein: 20-22% and metabolizable energy: 3.0-3.3 Kcal/g [30] and *ad libitum* access to clean drinking water during the period of experimentation. To reduce stress and maintain hygienic conditions, bedding material was renewed periodically, and cages were disinfected regularly. No more than four rats were housed in each cage to facilitate airflow and movement.

The animals were allowed to acclimatize to the laboratory for two weeks before starting any experimental procedures. All experimental protocols were approved by the Institutional Animal Care and Use Committee (IACUC). This study adhered to internationally accepted standards for animal research, following the 3Rs principle. The ARRIVE guidelines were employed for reporting experiments involving live animals, promoting ethical research practices. This study was approved by the Ethics and Policy Committee of the College of Veterinary Medicine, Al-Qadisiyah University, Iraq (No. 1180).

2.2. Chemicals and Reagents

Reproductive toxicity was induced in experimental animals by administering $CdCl_2$. We chose the natural polyphenolic compound Cm as a protective agent because of its well-characterized antioxidant and anti-inflammatory properties. Polymer-based Cm nanoparticles were prepared. All chemicals and reagents that were of analytical grade were purchased from commercial suppliers.

2.3. Synthesis of PCL/PVA-based Cm Nanoparticles

Cm-loaded nanoparticles were prepared by the emulsion–solvent evaporation method [31]. Briefly, the organic phase was obtained by dissolving polycaprolactone (PCL) in an organic solvent such as dichloromethane. Then, Cm was added to the same organic phase for encapsulation within the polymer matrix. Polyvinyl alcohol (PVA) was prepared in an aqueous solution to be used as a stabilizing surfactant. Under continuous stirring with a magnetic stirrer, the organic phase, including PCL and Cm, was gradually added to the aqueous phase containing PVA. The mixture was then homogenized using a high-speed blender to obtain a stable oil-in-water emulsion. Subsequently, the organic solvent was evaporated under continuous stirring, which provided efficient mixing and facilitated the formation of Cm-loaded nanoparticles. In this step, we centrifuged and washed the collected nanoparticles several times with distilled water to remove excess surfactant and unencapsulated drug. The recovered nanoparticles were later dried and stored under appropriate conditions for further use.

2.4. Preparation and Oral Gavage of Cm and Cm-loaded NPs

Native Cm suspension was prepared freshly before administration by dispersing Cm powder in a 0.5–1% carboxymethyl cellulose (CMC) solution under continuous magnetic stirring, followed by sonication for 10–15 minutes to ensure uniform dispersion. On the other hand, before administration of the NPs, the NP powder was reconstituted in 0.5% CMC and briefly sonicated to achieve a homogeneous suspension. Both native Cm and Cm-NP formulations were administered orally by gavage using a stainless-steel gavage needle at the required experimental dose according to the animal's body weight.

2.5. Evaluation of the Encapsulation Efficacy

The encapsulation efficiency and drug loading capacity were calculated by dissolving a given quantity of nanoparticles in an adequate solvent, followed by UV–visible spectrophotometric determination of Cm absorbance. Encapsulation efficiency was calculated as the ratio of Cm used at encapsulation to that detected in the supernatant [32].

2.6. Experimental Design

The experimental design followed the Organisation for Economic Co-operation and Development (OECD) Guideline 407 for a repeated-dose oral toxicity study [33]. Forty-eight adult female Wistar rats (aged 120–130 days and weighing 250–270 g) were used in this study. The animals were randomly allocated into six experimental groups (n = 8 per group). The current study evaluated the protective effects of native Cm and PCL/PVA/Cm NPs against Cd-induced reproductive toxicity.

2.6.1. Group T1 (Negative Control)

Animals were maintained under standard conditions and received no treatment throughout the experimental protocol.

2.6.2. Group T2 (Cd Control)

Rats were administered cadmium chloride ($CdCl_2$) at a dose of 30 mg/kg body weight/day orally for four weeks to induce reproductive toxicity [34].

2.6.3. Group T3 (Cm Control)

Intact rats were treated orally with native Cm at a dose of</mark> 0.207 mg/kg body weight/day for four weeks [35].

2.6.4. Group T4 (Cd + Cm)

Rats received both $CdCl_2$ (30 mg/kg/day) and native Cm (0.207 mg/kg/day) for four consecutive weeks.

2.6.5. Group T5 (Cm Nanoparticles Control)

Intact rats received orally administered synthesized PCL/PVA/Cm NPs at a dose of 0.207 mg/kg/day for four weeks.

2.6.6. Group T6 (Cd + Cm Nanoparticles)

Rats received $CdCl_2$ (30 mg/kg body weight/day) and PCL/PVA/Cm NPs (0.207 mg/kg body weight/day) for four weeks.

All treatments were administered *via* gastric gavage to ensure accurate dosing. Mortality, clinical signs of toxicity, and behavioral changes were monitored daily throughout the entire experiment.

2.7. Tissue Collection and Histopathological Examination

After an overnight (12 h) fast, female rats were euthanized at the end of the treatment period under appropriate anesthesia. The abdominal cavity was opened, and the reproductive organs, including the ovaries and uterus, were removed. The tissues were gently washed with physiological saline to remove blood and other contaminants and were fixed in 10% neutral buffered formalin for histomorphological analysis.

2.8. Histological Processing and Staining

Tissue samples fixed in formalin were processed according to standard histological procedures [36]. Tissues were dehydrated in a graded series of ethanol, cleared in xylene, and embedded in paraffin wax. Using a rotary microtome, paraffin blocks were cut into sections of 5 µm thickness. The sections were attached to glass slides and stained with hematoxylin and eosin (H&E) for the analysis of overall tissue morphology. Hematoxylin stains the cell nuclei blue, whereas eosin stains the cytoplasmic and extracellular components pink, thereby allowing the cellular structure to be easily visualized. Morphological changes in the ovarian follicles, uterine endometrium, and myometrial layers were assessed using the prepared slides under a light microscope. Changes in the histopathology were recorded and examined in relation to the experimental groups.

2.9. Statistical Analysis

The sample size of the experimental animals was determined based on previous studies with similar designs evaluating the toxicological effects of heavy metals and the protective role of plant extract-based formulations on reproductive and biochemical parameters. The calculation aimed to achieve sufficient statistical power to detect biologically significant differences among groups while minimizing the unnecessary use of animals, in accordance with ethical guidelines for animal research. Based on these assumptions, the minimum number of animals required per group was estimated to provide reliable and reproducible results.

All experimental data were statistically analyzed using GraphPad Prism (version 5). Results are expressed as mean ± standard deviation (SD). Statistical comparisons between experimental groups were performed using one-way ANOVA. When significant differences were observed, Tukey's multiple comparison test was used to identify differences between groups. Statistical significance was defined as a p-value of < 0.05 [37].

3. RESULTS

3.1. Ovaries

3.1.1. Microscopical Examination of Ovarian Sections

As compared to control female rats (Fig. **1**), Cd induced histopathological changes in the ovarian tissue. We observed that the ovary showed an irregular contour and a flattened germinal epithelium, numerous atretic follicles, degenerative corpus luteum structures, and chromatin condensation within ovarian cells, indicating apoptosis; furthermore, dilated and congested blood vessels were also observed (Fig. **2**).

Sections of the ovaries of Cm-treated female rats showed well-preserved histological structures. There were numerous primordial, primary, and secondary follicles with few *corpora lutea* observed, indicating active folliculogenesis and regular ovulation (Fig. **3**). Atretic follicles were scarce and remained within physiological ranges.

Cd and Cm co-administration appreciably preserved ovarian architecture. Histological examination showed clustered primordial and primary follicles, as well as multiple corpora lutea, suggesting ovulatory activity. However, atretic follicles were still visible, and secondary follicles were rarely observed; moreover, mild degeneration of luteal cells was also noted (Fig. **4**).

In contrast, ovarian sections obtained from female rats treated with PCL/PVA/Cm NPs (Fig. **5**) exhibited well-preserved histoarchitecture, characterized by an active ovarian cortex containing follicles at various developmental stages, including primordial, primary, secondary, and antral follicles, together with numerous healthy *corpora lutea*. These findings indicate enhanced follicular activity and normal ovarian function following PCL/PVA/Cm NPs administration.

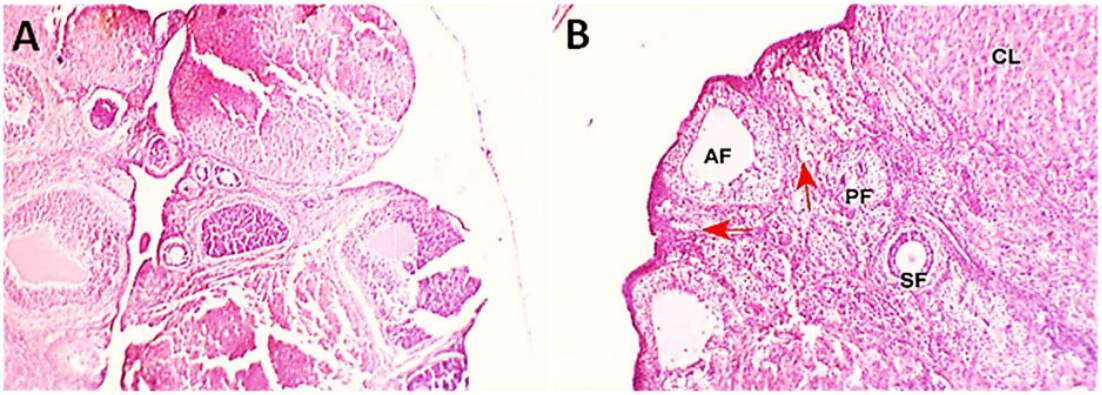

Fig. (1). Photomicrographs of ovarian tissue from a control group female rat showing the presence of numerous primordial (red arrows), primary (PF), and secondary follicles (SF), and several atretic follicles (AF), and multiple *corpora lutea* (CL), indicating active folliculogenesis and ovulatory activity. **A**) H&E, X40. **B**) H&E, ×100.

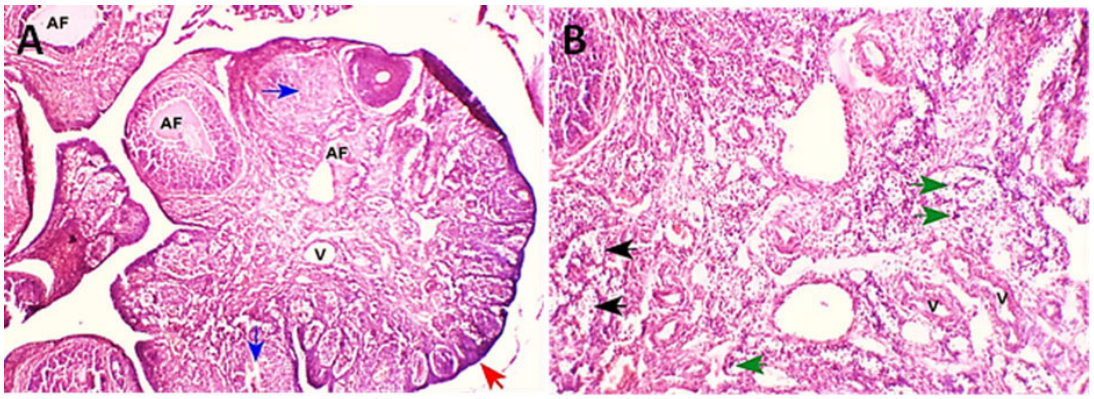

Fig. (2). Photomicrographs from the Cd-treated group (T2 group). **A**) shows an ovary with an irregular contour and a flattened squamous germinal epithelium (red arrow). Numerous atretic follicles (AFs) are evident, along with degenerated *corpus luteum* structures (blue arrows). Dilated and congested blood vessels are also observed in the cortical region (V). H&E, X40. **B**) shows irregular distribution of ovarian cells (black arrows), with chromatin condensation in the nuclei highlighted by green arrows. H&E, X100.

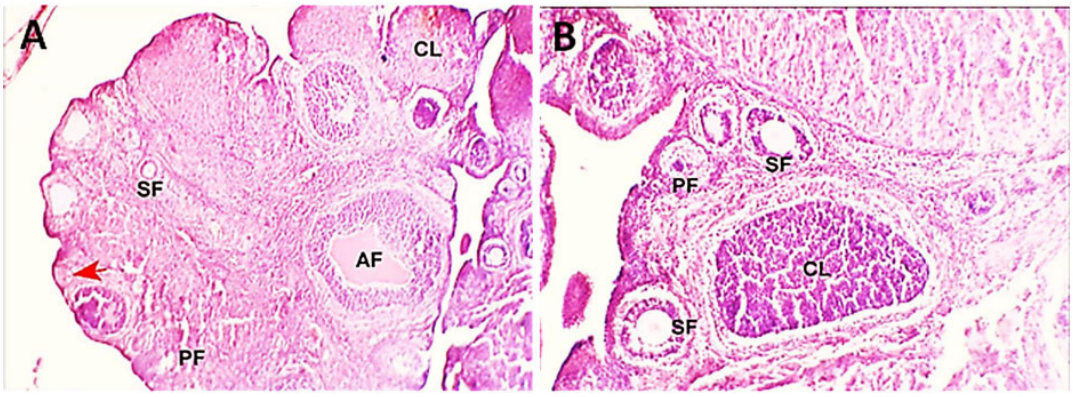

Fig. (3). Photomicrographs of ovarian tissue from the Cm-treated group (T3) showing the presence of numerous primordial (red arrows), primary (PF), and secondary follicles (SF), and several atretic follicles (AF), and multiple *corpora lutea* (CL), indicating active folliculogenesis and ovulatory activity. **A**) H&E, ×40. **B**) H&E, ×100.

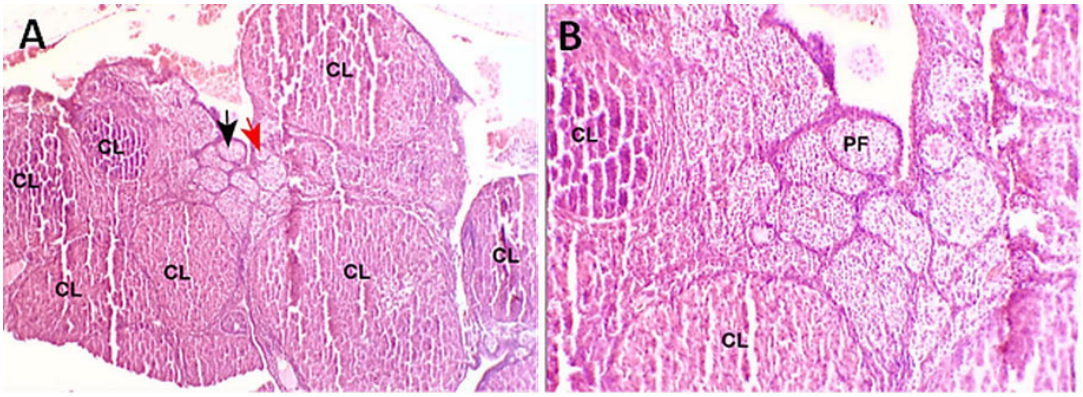

Fig. (4). Photomicrographs of the ovarian tissues from the Cd+Cm-treated group (T4). **A**) reveals numerous clustered primordial (red arrows) and primary follicles (black arrows), along with multiple *corpora lutea* (CL), indicating a regenerative or luteinized ovarian condition. H&E, X40. **B**) reveals clustered primary follicles (PF), along with multiple *corpora lutea* (CL), indicating a regenerative or luteinized ovarian condition. H&E, X100.

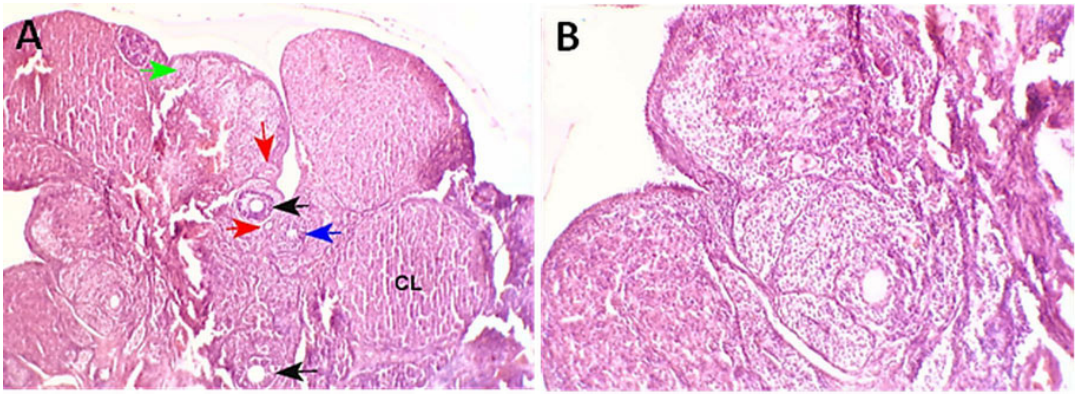

Fig. (5). Histological sections of the ovarian tissues from the PCL/PVA/Cm NPs –treated group (T5). **A**) displays numerous primordial (green arrow), primary (red arrows), secondary (blue arrow), and antral follicles (black arrows) along with multiple *corpora lutea* (CL), indicating active folliculogenesis and sustained ovulatory activity. H&E, x40. **B**) shows an active cortical region containing various stages of immature follicles. H&E, 100X.

Notably, the ovaries of female rats co-treated with $CdCl_2$ and PCL/PVA/Cm NPs (Fig. **6**) demonstrated marked histological improvement, with a highly active ovarian cortex containing follicles at all stages of development, ranging from primordial to mature Graafian follicles. The Graafian follicles were clearly identified by the presence of a distinct basement membrane, well-organized granulosa cell layers, an intact *zona pellucida*, and a morphologically normal oocyte. These observations suggest that PCL/PVA/Cm NPs effectively attenuated Cd-induced ovarian injury and promoted the restoration of normal folliculogenesis.

As summarized in Table **1**, the PCL/PVA/Cm NPs-treated group exhibited the most promising ovarian histological profile among experimental groups. This profile was characterized by active folliculogenesis, evidenced by profuse developing follicles, multiple healthy *corpora lutea*, minimal follicular atresia, and preserved vascular integrity. Together, these findings suggest that administration of Cm-loaded NPs alone provides higher preservation of ovarian morphology and enhanced ovarian functional capacity. Conversely, the Cd-exposed group showed the most severe histopathological changes, including marked suppression of folliculogenesis, extensive follicular atresia, degeneration of *corpora lutea*, and distinct vascular impairment, indicating the deleterious effects of Cd exposure on ovarian tissue.

Although both the Cd + Cm and Cm-treated groups revealed substantial histological recovery, reflected by improved follicular development, reduced atresia, and restoration of ovarian activity, their overall histological status remained slightly less than that observed in the PCL/PVA/Cm NPs-treated group. Nevertheless, the Cd + Cm group showed slight restoration of normal ovarian architecture, highlighting the protective effect of curcumin against Cd-induced ovarian toxicity.

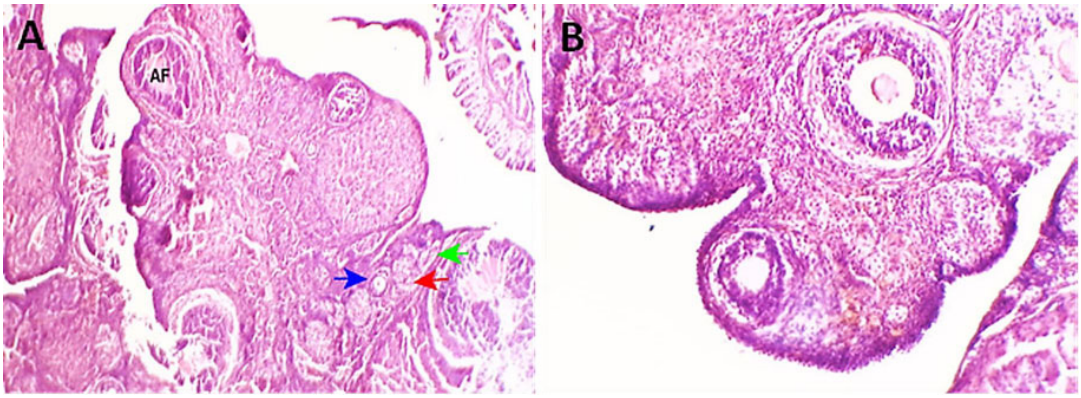

Fig. (6). Histological sections of ovarian tissues from the combination treatment of Cd and PCL/PVA/Cm NPs-treated group (T6) reveal an active ovarian cortex containing all developmental stages of follicles, including primordial, primary, secondary, and Graafian follicles. **A**) H&E, x40. **B**) H&E, x100.

Table 1. Histological assessment of ovarian activity in experimental groups.

Groups	Folliculogenesis	*Corpora Lutea*	Atresia	Vascular Integrity	Overall Histological Status
T1 Control	Active (Prim., Sec.)	Multiple, Normal	Minimal	Intact	Best-preserved ovarian structure
T2 Cd	Absent	Degenerated	Extensive	Compromised	Severely damaged
T3 Cm Only	Active (Prim., Sec.)	Multiple, Normal	Minimal	Intact	Best-preserved ovarian structure
T4 Cd+Cm	Partial	Present	Moderate	Partially preserved	Moderately affected (partial recovery)
T5 PCL/PVA/Cm Nps	Active (Prim., Sec., Antral)	Multiple, Normal	Minimal	Preserved	Enhanced folliculogenesis with preserved architecture
T6 Cd+PCL/PVA/Cm Nps	Active (Prim., Sec., Graafian)	Multiple, Mature (CLs)	Minimal	Restored	Normal histology; marked recovery from Cd toxicity

Note: T1: treated with distilled water; T2: treated with $CdCl_2$; T3: treated with native Cm; T4: treated with combination of $CdCl_2$ and Cm; T5: treated with PCL/PVA/Cm NPs; T6: treated with combination of $CdCl_2$ and PCL/PVA/Cm NPs.

Table 2. Histopathological scoring of ovarian tissue between experimental groups.

Group	Folliculogenesis	*Corpora Lutea*	Follicular Atresia*	Vascular Integrity	Overall Score **	Histological Interpretation
T1 Control	3.0 ± 0.0^a	3.0 ± 0.0^a	3.0 ± 0.0^a	3.0 ± 0.0^a	3.0 ± 0.0^a	Normal ovarian architecture
T2 Cd	0.0 ± 0.0^c	0.0 ± 0.0^c	0.0 ± 0.0^c	1.0 ± 0.0^c	0.25 ± 0.50^c	Severe ovarian damage
T3 Cm	3.0 ± 0.0^a	3.0 ± 0.0^a	3.0 ± 0.0^a	3.0 ± 0.0^a	3.0 ± 0.0^a	Normal ovarian histology
T4 Cd + Cm	2.0 ± 0.0^b	2.0 ± 0.0^b	2.0 ± 0.0^b	2.0 ± 0.0^b	2.0 ± 0.0^b	Moderate recovery
T5 PCL/PVA/Cm NPs	3.0 ± 0.0^a	3.0 ± 0.0^a	3.0 ± 0.0^a	3.0 ± 0.0^a	3.0 ± 0.0^a	Enhanced folliculogenesis
T6 Cd + PCL/PVA/Cm NPs	3.0 ± 0.0^a	3.0 ± 0.0^a	3.0 ± 0.0^a	3.0 ± 0.0^a	3.0 ± 0.0^a	Marked protection and restoration

Note: *Higher score indicates lower follicular atresia.
** Mean score calculated from the four histological parameters (Mean ± SD).
Data are presented as mean ± SD of semi-quantitative histological scores (0–3). Different superscript letters (a, b, c) in the same column indicate significant differences and are determined by post hoc analysis, $P < 0.05$. An upper score indicates better ovarian histological preservation with less follicular atresia.
T1: treated with distilled water; T2: treated with $CdCl_2$; T3: treated with native Cm; T4: treated with a combination of $CdCl_2$ and Cm; T5: treated with PCL/PVA/Cm NPs; T6: treated with a combination of $CdCl_2$ and PCL/PVA/Cm NPs.

3.1.2. Semi-quantitative Histopathological Scoring of Ovarian Tissue

For Semi-quantitative analysis, the evaluated parameters involved folliculogenesis (assessed based on the presence of follicles at different developmental stages), *corpora lutea* integrity, follicular atresia (reverse-scored; whereby a higher score indicate lower degree of atresia), vascular integrity, and the overall histological score, which was calculated as the mean of all measured parameters) (Table 2).

The control group (T1) represented the physiological baseline condition and exhibited normal ovarian histoarchitecture, characterized by active folliculogenesis, the presence of multiple healthy *corpus lutea*, minimal follicular atresia, and intact vascular structures. In contrast, Cd exposure induced the most severe histopathological alterations in ovarian tissue. Histological examination of the Cd-treated group (T2) displayed a marked impairment in folliculogenesis with numerous follicles undergoing advanced atresia and degenerated *corpora lutea* along with vascular congestion, resulting in the lowest histological score among experimental groups. This is likely due to the severe gonadal toxic effect of Cd.

Treatment with Cm alone (T3) preserved normal ovarian morphology comparable to the control group. Histological examination revealed a well-maintained ovarian architecture characterized by the presence of numerous primordial, primary, and secondary follicles, together with structurally intact *corpora lutea*, suggesting that Cm administration does not have an adverse effect on ovarian histology and effectively maintains normal ovarian function. Partial protection against Cd toxicity was observed in the Cd + Cm group (T4). Ovarian sections exhibited resumed follicular development, as demonstrated by the presence of primordial and primary follicles and several *corpora lutea*. However, histopathological alterations persisted, including follicular atresia and mild luteal degeneration. These findings suggest that native curcumin exerted a moderate restorative effect against cadmium-induced ovarian damage, although complete histological recovery was not achieved.

The PCL/PVA/Cm NPs-treated group (T5) exhibited the most significant ovarian histological profile among experimental groups. Sections from ovaries showed active stages of folliculogenesis characterized by the presence of numerous primordial, primary, secondary, and antral follicles, along with multiple healthy *corpora lutea* and preserved vascular structures. The ovarian architecture appeared highly organized and functionally active, indicating increased bioavailability, biological activity of Cm, and its encapsulation to nano-scale. The Cd + PCL/PVA/Cm NPs (T6) group exhibited almost normal ovarian architecture, comparable to that found in the control groups. Ovarian sections exhibited normal follicular progression across different developmental stages, including abundant intact Graafian follicles, preserved *corpora lutea*, and intact vascular networks, accompanied by minimal follicular atresia. The substantial restoration of ovarian architecture and follicular integrity observed in this group indicates a pronounced protective effect against Cd-induced ovarian damage. Collectively, these findings confirm the enhanced therapeutic efficacy of PCL/PVA/Cm NPs in mitigating Cd-induced ovarian toxicity and preserving ovarian structure and function.

3.2. Uteri

3.2.1. Microscopical Examination of Uteri Sections

Compared with control female rats (Fig. **7**), histopathological examination of the uterus from the Cd-treated female rats (Fig. **8**) revealed marked degenerative and inflammatory alterations. The endometrial epithelium appeared markedly attenuated and exhibited a decline in cellular density and a reduced number of uterine glands. In several uterine sections, glandular atrophy was evident, accompanied by lymphocytic infiltration within the endometrial stroma. Moreover, congested blood vessels and apoptotic changes in the luminal epithelium were observed, indicating tissue injury and inflammatory response.

In comparison to Cm-treated female rats (Fig. **9**), uterine sections from the Cd + Cm-treated group (Fig. **10**) showed partial amelioration of Cd-induced pathological alterations. Histological examination exhibited a thicker columnar epithelial layer with numerous uterine glands and moderate regeneration of endometrial architecture. Nevertheless, residual pathological changes were still evident in several sections, including vascular congestion, focal hemorrhage, inflammatory cell infiltration, and partial disruption of the myometrial organization.

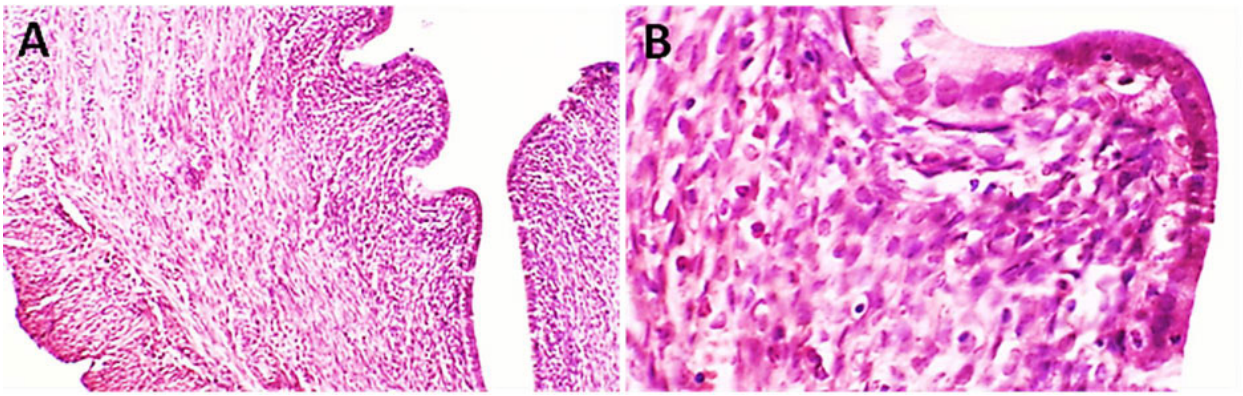

Fig. (7). Photomicrographs of uterine tissue from a control group female rat (T1). **A**) A uterus with normal structure. H&E, ×100. **B**) shows a uterus with normal structure of the endometrial layer. H&E, ×400.

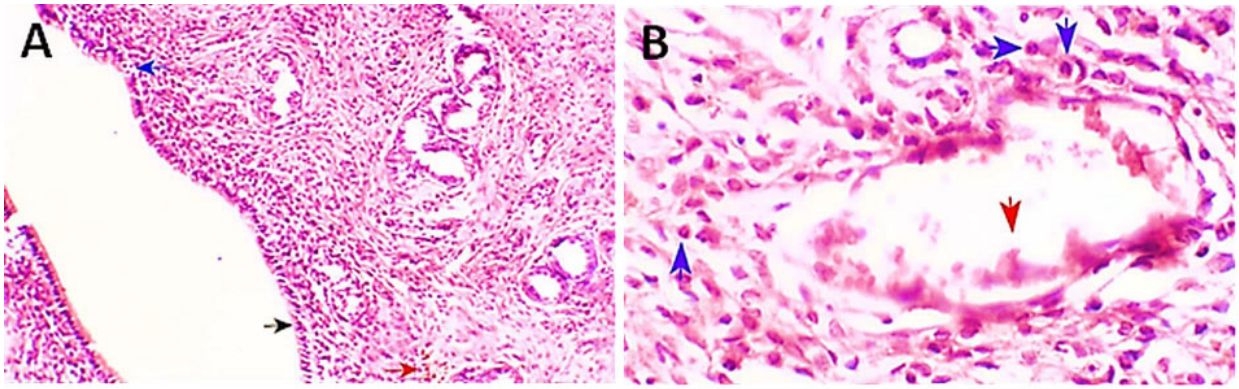

Fig. (8). Photomicrograph of uterine tissue from Cd-treated group female rat (T2). **A**) shows a uterus with a thin epithelial layer (black arrow), apoptosis in the luminal epithelium (blue arrow) with lymphocytic infiltration (red arrow). H&E, X100. **B**) shows a uterus with congested blood vessels (red arrow) and infiltration of inflammatory cells (blue arrows). H&E, X400.

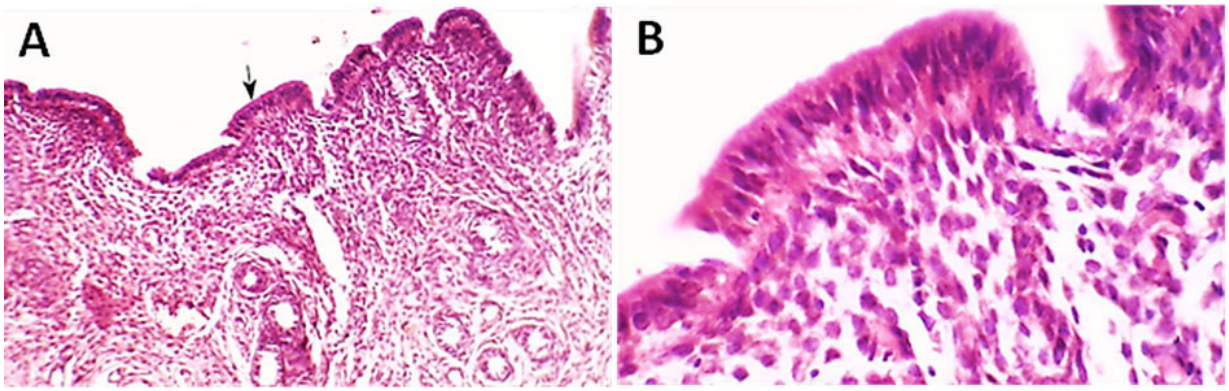

Fig. (9). Photomicrograph of uterine tissue from the Cm-treated group female rat (T3) shows a uterus with a thick columnar epithelial layer (black arrow). **A**) H&E, X100, **B**) H&E, X400.

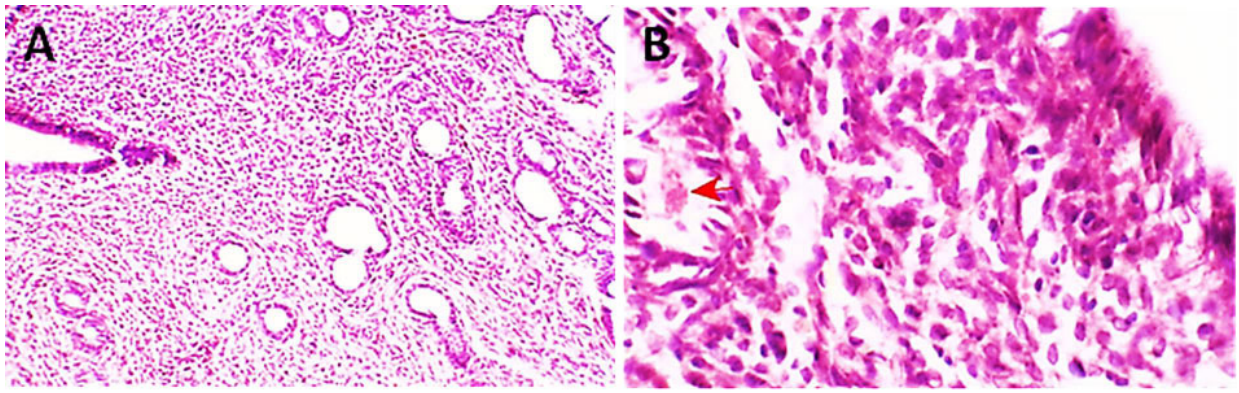

Fig. (10). Photomicrograph of uterine tissue from the Cd + Cm-treated group female rat (T4) shows a uterus with hemorrhage (red arrow) and disruption of the myometrial architecture. **A**) H&E, X100, **B**) H&E, X400.

The PCL/PVA/Cm NP–treated group of female rats (Fig. **11**) exhibited well-preserved uterine architecture, characterized by a well-organized endometrial epithelial layer, numerous well-developed uterine glands, and an intact myometrium without evidence of congestion, necrosis, or inflammatory infiltration. Similarly, the Cd+ PCL/PVA/Cm NPs–treated group of female rats (Fig. **12**) displayed a remarkable improvement in uterine morphology, exhibiting nearly normal histological structure comparable to that of the control group. The endometrial epithelium was intact and well-organized, with multiple active uterine glands and an absence of inflammation or degeneration changes.

The histopathological examination of uterine tissues (Table **3**) demonstrated normal histoarchitectural organization in the control group (T1), characterized by an intact endometrial epithelial lining, well-developed uterine glands, and normal myometrial architecture. In contrast, the T2 group (Cd-treated) exhibited significant degenerative and inflammatory changes, including attenuation of the epithelial lining, glandular atrophy, lymphocytic infiltration, vascular congestion, and apoptotic changes of luminal epithelium. Treatment with Cm alone (T3) maintained normal uterine morphology, characterized by a well-developed columnar epithelial layer and intact glandular structures. Co-administration of Cd and curcumin (T4) resulted in partial histological recovery of the uterine tissue; however, residual pathological lesions, including vascular congestion, hemorrhage, inflammatory infiltration, and focal disruption of the myometrial layer, remained evident. Histological examination of the PCL/PVA/Cm NPs-treated group (T5) demonstrated well-preserved uterine architecture comparable to that of the control group, with no apparent pathological alterations. Notably, the Cd + PCL/PVA/Cm NPs group (T6) exhibited substantial amelioration of Cd-induced uterine injury, as evidenced by the restoration of normal uterine morphology, re-establishment of endometrial integrity, and the presence of numerous active uterine glands, resulting in a histological appearance closely resembling that of the control group.

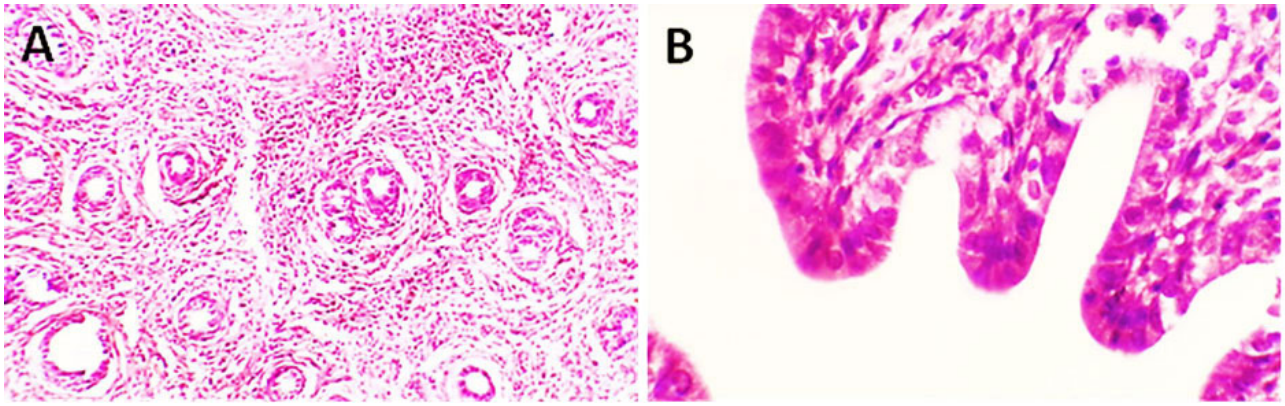

Fig. (11). Photomicrograph of uterine tissue from the PCL/PVA/Cm NPs –treated group female rat (T5) shows a uterus with normal structure of the endometrial layer and glands. **A**) H&E, X100, **B**) H&E, X400.

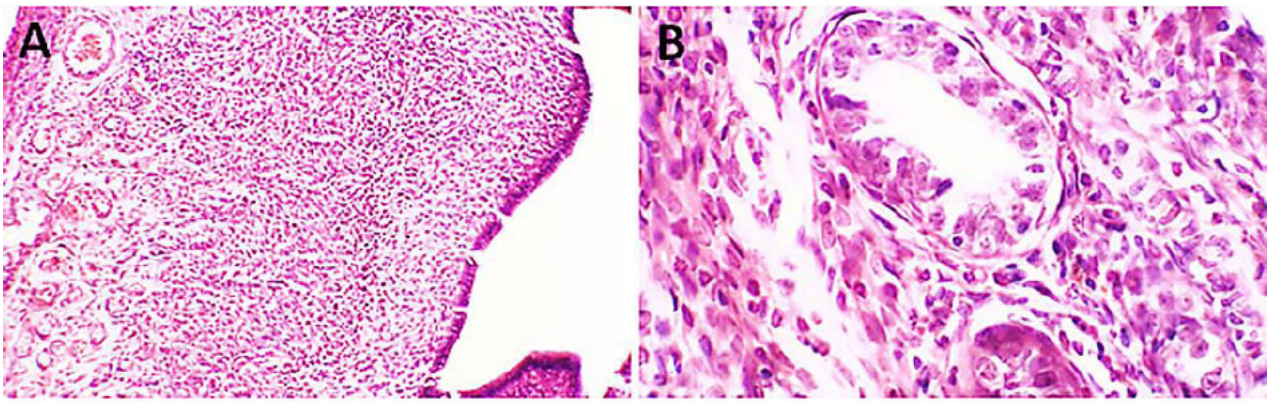

Fig. (12). Photomicrograph of uterine tissue from the PCL/PVA/Cm NPs –treated group female rat (T6) shows a uterus with normal structure of the endometrial layer and active endometrial glands. **A**) H&E, X100, **B**) H&E, X400.

Table 3. Histopathological alterations in uterine tissues of experimental female rats.

Group	Treatment	Histopathological Findings
T1	Control	Normal uterine histological structure, including intact endometrial epithelium, well-ordered arrangement of endometrium, and presence of abundant normal uterine glands with intact myometrium, showing no inflammatory infiltration and vascular congestion.
T2	Cd	Histopathological changes were evident, which included thinning of the endometrial epithelial lining, reduced cellular density, decreased number of uterine glands with glandular atrophy, lymphocytic infiltration in the endometrial stroma, congested blood vessels, and apoptotic changes in the luminal epithelium.
T3	Cm	Less rigid uterine lining with columnar epithelium and preserved endometrial architecture, including functional uterine glands.
T4	Cd + Cm	Marked improvement of Cd-induced lesions, with mild regeneration of endometrial architecture and increased numbers of glands; nevertheless, some sections showed vascular congestion, hemorrhage, inflammatory cell infiltration, and myometrial structure disturbance.
T5	PCL/PVA/Cm NPs	Normal uterine histology showing regular endometrial epithelium, many functional uterine glands, and intact myometrium free from congestion, necrosis, and inflammatory infiltration.
T6	Cd + PCL/PVA/Cm NPs	A significant recovery with almost normal uterine structure like the control group, including intact endometrial epithelium, properly organized stromal tissues and several actively producing uterine glands without any detectable inflammatory or degenerative changes

Note: T1: treated with distilled water; T2: treated with $CdCl_2$; T3: treated with native Cm; T4: treated with a combination of $CdCl_2$ and Cm; T5: treated with PCL/PVA/Cm NPs; T6: treated with a combination of $CdCl_2$ and PCL/PVA/Cm NPs.

3.2.2. Semi-quantitative Histopathological Scoring of Uterine Tissue

Semi-quantitative analysis of uterine histopathological alterations (Table **4**) demonstrated that the Cd-treated group (T2) exhibited the highest severity of tissue lesions, characterized by marked epithelial degeneration, moderate glandular atrophy, inflammatory cell infiltration, and pronounced vascular congestion. In contrast, the control group (T1) showed normal uterine histoarchitecture with no detectable pathological changes. Administration of Cm alone (T3) preserved uterine histology comparable to that of the control group. Co-treatment with Cd and Cm (T4) resulted in partial improvement, with mild epithelial degeneration and glandular atrophy accompanied by moderate vascular congestion still evident. Notably, rats treated with PCL/PVA/Cm NPs (T5) exhibited well-preserved uterine architecture without observable histopathological lesions. Furthermore, the Cd + PCL/PVA/Cm NPs group (T6) showed near-complete restoration of uterine morphology, with histological scores comparable to those of the control group, indicating a substantial protective and restorative effect of nano-encapsulated Cm against Cd-induced uterine toxicity.

3.2.3. Morphometric Evaluation of the Uteri

A morphometric examination of the uterus was conducted to quantitatively evaluate the structural changes induced by $CdCl_2$ exposure and the potential protective effects of Cm and Cm-loaded nanoparticles. Measurements focused on endometrial and myometrial thickness, which served as key markers of uterine structural and functional integrity (Table **5** and Fig. **13**).

The control group showed normal morphometric structure, characterized by a well-developed endometrium, regularly distributed uterine glands, and a uniformly organized myometrial layer. These findings reflect normal uterine architecture and estrogen-dependent physiological responsiveness.

Table 4. Numerical semi-quantitative scores of uterine histopathological alterations in experimental female rats.

Group	Treatment	Epithelial Degeneration	Glandular Atrophy	Inflammatory Cell Infiltration	Vascular Congestion / Hemorrhage	Myometrial Disruption
T1	Control	0.00 ± 0.00^{a}	0.00 ± 0.00^{a}	0.00 ± 0.00^{a}	0.00 ± 0.00^{a}	0.00 ± 0.00^{a}
T2	Cd	3.00 ± 0.00^{c}	2.00 ± 0.00^{c}	2.00 ± 0.00^{c}	2.00 ± 0.00^{c}	1.00 ± 0.00^{c}
T3	Cm	0.00 ± 0.00^{a}	0.00 ± 0.00^{a}	0.00 ± 0.00^{a}	0.00 ± 0.00^{a}	0.00 ± 0.00^{a}
T4	Cd + Cm	1.00 ± 0.00^{b}	1.00 ± 0.00^{b}	1.00 ± 0.00^{b}	2.00 ± 0.00^{b}	1.00 ± 0.00^{b}
T5	PCL/PVA/Cm NPS	0.00 ± 0.00^{a}	0.00 ± 0.00^{a}	0.00 ± 0.00^{a}	0.00 ± 0.00^{a}	0.00 ± 0.00^{a}
T6	Cd + PCL/PVA/Cm NPs	0.00 ± 0.00^{a}	0.00 ± 0.00^{a}	0.00 ± 0.00^{a}	0.00 ± 0.00^{a}	0.00 ± 0.00^{a}

Note: Values are presented as mean ± SEM. ep means in the same column with different superscripts (a, b, c) are significantly different from each other ($p < 0.05$); one-way ANOVA followed by Tukey's post-hoc test.

T1: treated with distilled water; T2: treated with $CdCl_2$; T3: treated with native Cm; T4: treated with a combination of $CdCl_2$ and Cm; T5: treated with PCL/PVA/Cm NPs; T6: treated with a combination of $CdCl_2$ and PCL/PVA/Cm NPs.

Table 5. Summary of uterine structural morphology.

Group	Treatment	Interpretation
T1	Distilled Water	Normal uterine architecture
T2	$CdCl_2$	Marked uterine atrophy
T3	Cm	Near-normal morphology
T4	$CdCl_2$ + Cm	Partial recovery
T5	PCL/PVA/Cm NPs	Preserved uterine structure
T6	$CdCl_2$ + PCL/PVA/Cm NPs	Significant protection

Note: T1: treated with distilled water; T2: treated with $CdCl_2$; T3: treated with native Cm; T4: treated with a combination of $CdCl_2$ and Cm; T5: treated with PCL/PVA/Cm NPs; T6: treated with a combination of $CdCl_2$ and PCL/PVA/Cm NPs.

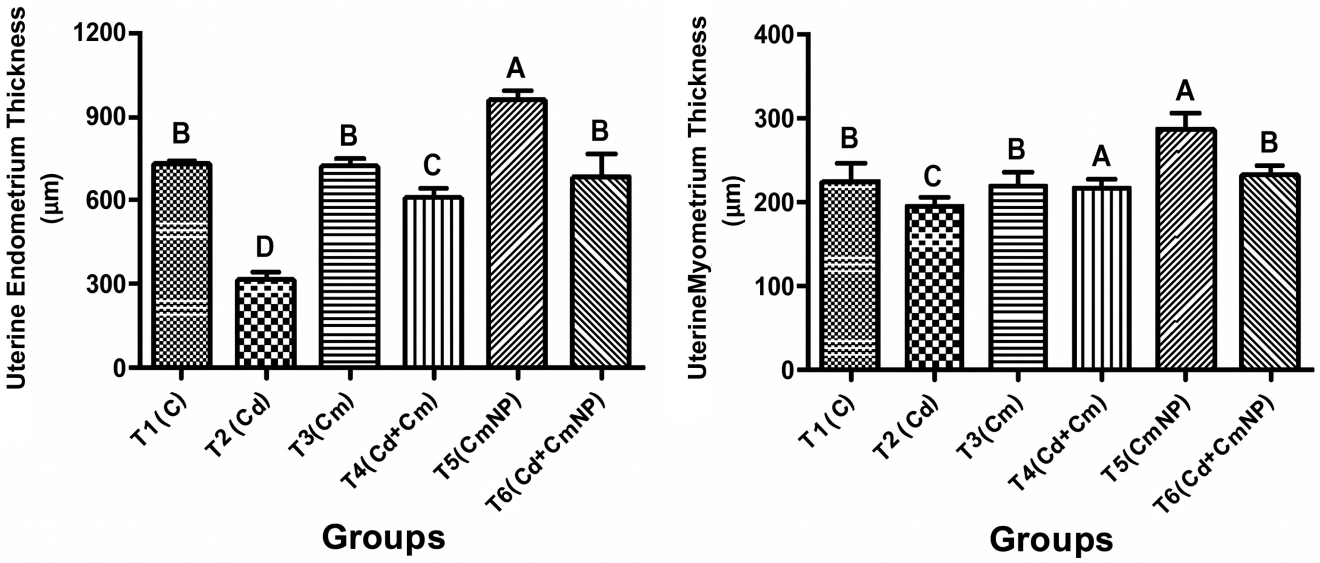

Fig. (13). (**A** and **B**) Uterine endometrium and myometrium thickness (µm) of female rats after 4 weeks of supplementation with distilled water (**T1**), $CdCl_2$ (**T2**), Cm (**T3**), combination of $CdCl_2$ and Cm (**T4**), PCL/PVA/Cm NPs (**T5**), and combination of $CdCl_2$ and PCL/PVA/Cm NPs (**T6**). A) H&E, X100, B) H&E, X400.
$CdCl_2$: Cadmium chloride; **Cm**: Cucumin; **PCL**: Polycaprolactone; **PVA**: Polyvinyl alcohol; **NPs**: Nanoparticles.
The values were presented as mean ± standard deviation.
The different letters denote significant differences ($p<0.05$) between groups.

Exposure to $CdCl_2$ resulted in a significant decrease in both endometrial and myometrial thickness, pronounced uterine atrophy, and structural deterioration. These reductions may be attributed to impaired hormonal responsiveness and Cd-induced tissue damage.

Treatment with Cm alone preserved uterine morphometric dimensions at levels comparable to those of the control, suggesting good biocompatibility and a possible modulatory effect on estrogen-dependent uterine function. Furthermore, co-administration of Cm with $CdCl_2$ markedly reduced the Cd-mediated reduction in uterine thickness, representing partial recovery of uterine architecture.

Similarly, treatment with PCL/PVA/Cm NPs maintained or enhanced both endometrial and myometrial thickness compared with the control group. Notably, co-treatment with $CdCl_2$ and Cm-loaded NPs resulted in better improvement in uterine morphometric parameters than free Cm, demonstrating a higher bioavailability and protective efficacy of the nanoformulation.

Overall, these morphometric observations confirm the deleterious effects of $CdCl_2$ on the structure of uterine tissue, while Cm- especially in its nanoparticle formulation- effectively mitigated these alterations and preserved uterine morphometric integrity.

Quantitative evaluation of the uterine morphometric parameters revealed marked differences between groups (Fig. **13**).

4. DISCUSSION

Cd is known to accumulate in multiple organs, such as the ovary and the uterus, impairing normal reproductive physiological functions. Cd acts as an endocrine-disrupting chemical capable of disrupting the hypothalamic–pituitary–gonadal axis and interfering with folliculogenesis and steroidogenesis, as demonstrated by

both experimental and epidemiological studies [2, 4]. In female reproductive tissues, Cd-induced toxicity is predominantly brought about *via* oxidative stress, mitochondrial dysfunction, and activation of apoptotic signaling pathways, which drastically affect follicular development and uterine integrity [38]. These mechanisms are consistent with the histopathological changes noted in this study, including follicular atresia, *corpora lutea* degeneration, vascular congestion, and uterine epithelial degeneration.

Due to its high metabolic activity and extensive vascular supply, ovarian tissue is particularly susceptible to Cd-induced toxicity. Cd exposure promotes the generation of ROS formation and lipid peroxidation while suppressing endogenous antioxidant defense systems, including superoxide dismutase and catalase [39]. Excessive oxidative stress induces granulosa cell apoptosis and oocyte damage, resulting in impaired folliculogenesis and increased luteal atresia. Consistent with these mechanisms, the present findings revealed marked ovarian damage in the Cd-challenged group, characterized by irregular ovarian architecture, degenerated germinal epithelium, multiple atretic follicles, degenerated corpora lutea, and vascular congestion. These observation agrees with earlier studies reporting Cd exposure causes follicular degeneration and dysregulation of ovarian architecture [40, 41].

Semi-quantitative histopathological scoring further confirmed the severe gonadotoxic effects of Cd. In the Cd-treated group, folliculogenesis was virtually abolished, and extensive follicular atresia coupled with compromised vascular integrity resulted in the lowest histological scores of all experimental groups treated with Cd. These remarkable changes may be attributed to Cd-induced granulosa cell apoptosis and inhibition of ovarian steroidogenesis, resulting in follicular arrest and degeneration [3, 10]. Previous studies have demonstrated that Cd exposure promotes cellular death and ovarian tissue degeneration [9], findings that are in agreement with the histopathological observations of the present study. Collectively, these results provide compelling evidence that Cd is a potent reproductive toxicant capable of impairing ovarian function and fertility.

In addition to its damage to ovarian tissue, Cd also has harmful effects on uterine tissue. Histopathological examination of uterine sections from Cd-exposed rats demonstrated reduced thickness of the endometrial epithelium and glandular atrophy accompanied by inflammatory cell infiltration, vascular congestion, and apoptotic alterations in luminal epithelium. These observations are consistent with previous studies demonstrating that Cd disrupts uterine architecture and reduces *via* disrupting estrogen signaling pathways and creating oxidative stress [5, 42]. Morphometric assessment further confirmed Cd-induced uterine atrophy, as evidenced by significant reductions in both endometrial and myometrial thickness. Such structural advancements are likely indices of downgraded hormonal responsiveness and tissue remodeling processes in the uterus.

Extensive evidence has reported that Cm possesses potent antioxidant and anti-inflammatory properties, enabling it to neutralize ROS, inhibit inflammatory mediators, and regulate multiple cellular signaling pathways involved in oxidative stress and apoptosis [12, 43]. Several experimental studies have shown that Cm protects against heavy metal-induced reproductive toxicity. Cm Supplementation has demonstrated the ability to restore antioxidant defenses, maintain follicular development, and enhance reproductive hormone balance [15, 44].

In agreement with these reports, the current study demonstrated that administration of Cm alone maintained normal ovarian and uterine histology, demonstrating positive reproductive effects on gonads. However, native Cm showed only partial protective effects when given in conjunction with Cd. Histopathological results reflected moderate improvement in ovarian morphology in the Cd + Cm group, characterized by the presence of primordial and primary follicles along with a few *corpora lutea*. Nevertheless, atretic follicles and mild luteal degeneration were still observed, indicating incomplete recovery. This partial protection could be described with previous studies which reported Cm attenuates oxidation damage; however was unable to restore Cd-induced tissue injury completely [45]. The limited therapeutic efficacy of native Cm is largely attributed to its poor aqueous solubility, rapid metabolism, and low systemic bioavailability [20].

To mitigate these pharmacokinetic limitations, nanotechnology-based delivery systems have been established to improve Cm bioavailability and therapeutic efficacy. Nanoparticle encapsulation of Cm enhances its solubility, stability, cellular uptake, and tissue distribution [22, 23]. Nano-Cm formulations exhibited better antioxidant, anti-inflammatory and cytoprotective activities than those of native Cm [28, 46]. These benefits render Cm nanoparticles as promising therapeutic candidates for the prevention of oxidative stress-induced tissue damage.

This study provides clear evidence that PCL/PVA/Cm NPs exert a greater protective effect against Cd-induced reproductive toxicity. Ovarian sections from the nanoparticle-treated groups showed well-preserved architecture, active folliculogenesis, multiple healthy *corpora lutea*, and intact vascular structures. Notably, the Cd + PCL/PVA/Cm NPs group exhibited almost normal ovarian histology with follicles at all developmental stages, including mature Graafian follicles. These findings indicate that nanoparticle-based delivery of Cm protects cells against Cd toxicity in a more effective way.

Likewise, uterine histology of the nanoparticle-treated groups showed near- complete restoration of normal tissue architecture. The endometrial epithelium remained intact and was accompanied by numerous functional glands and well-organized stromal structures. Morphometric quantification further corroborated these findings, showing no significant difference in endometrial or myometrial thickness relative to that of control animals. These findings suggest that Cm-loaded nanoparticles

effectively preserve uterine structural integrity and protect against Cd-induced uterine damage.

The improved effectiveness of nano-Cm exhibited in this study might result from various mechanisms. First, by the enclosure of Cm into nanoparticles improves the bioavailability and targeted delivery of Cm, allowing higher amounts to be accumulated at sites of tissue injury [22]. Second, nano-Cm enhances the intracellular antioxidant activity, thereby reducing ROS creation and lipid peroxidation associated with Cd toxicity [23]. Third, nano-formatted Cm may synergistically modulate key molecular pathways involved in cellular survival, including the Nrf2 antioxidant pathway and PI3K/Akt signaling cascade that are critical protective responses for ovarian cells against apoptosis [47, 48]. Overall, these mechanisms likely account for the better therapeutic performance of nano-Cm in relation to its native counterpart.

Overall, the present study demonstrates that Cd causes severe structural and functional impairment of female reproductive organs through oxidative stress, apoptosis, and disruption of key cellular signaling pathways including Nrf2 and PI3K/Akt. Although native Cm provides partial protection against these toxic effects, nano-formulated Cm exhibits significantly stronger therapeutic efficacy. The improved bioavailability and enhanced biological activity of Cm nanoparticles allow more efficient modulation of oxidative stress and apoptosis pathways, leading to effective restoration of ovarian and uterine architecture.

The findings of the present study provide initial and promising preliminary evidence supporting the potential application of nano-curcumin-based therapeutic strategies in mitigating Cd-induced reproductive toxicity. Given that female rats represent a well-established mammalian model with considerable physiological relevance to both human and veterinary reproductive systems, further investigations in humans and field animal species are warranted to validate the translational potential of these findings.

5. LIMITATIONS

The present study has several limitations. First, the investigation was conducted using a single experimental model, which may limit the generalizability of the findings to human populations. Second, the long-term safety profile and potential toxicological effects of the nanoparticle delivery system were not evaluated. Furthermore, molecular mechanisms underlying the improved protective efficacy of nano-curcumin were not fully elucidated. Finally, the dose-response relationships, biodistribution, and pharmacokinetic properties of nano-Cm have not been comprehensively studied. Future studies should address these limitations to further validate the therapeutic potential and safety of nano-curcumin formulations.

CONCLUSION

The current research illustrates that Cd toxicity has greatly disrupted the structural and functional integrity of female reproductive organs, particularly the ovaries and uteri, as evidenced by impaired folliculogenesis in addition to reduced endometrial and myometrial thickness. Native Cm exhibited a protective effect against toxicity induced by Cd; however, its efficacy was only partial, likely due to its poor solubility, rapid metabolism, and low bioavailability. In contrast, Cm nanoparticles embedded within a PCL/PVA delivery system provided significantly better protection, preserving ovarian architecture and folliculogenesis in addition to restoring uterine structure toward normal. Such improved efficacy could be linked to improved bioavailability, stability, and cellular penetration of the nano-formulated compound. Overall, nano-Cm has significant therapeutic potential against heavy-metal-induced reproductive toxicity. Nanoparticle-based formulations exhibit enhanced pharmacokinetic and biological characteristics compared to native Cm, highlighting the potential of using nanotechnology-based antioxidant approaches to minimize reproductive toxicity caused by environmental toxicants.

AUTHORS' CONTRIBUTIONS

The authors confirm contribution to the paper as follows: J.A.A.A.S.: Study conception and design; M.N.A.A.M.: Data collection; J.A.A.A.S and M.N.A.A.M.: Analysis and interpretation of results; J.A.A.A.S.: Draft manuscript. Both authors reviewed the results and approved the final version of the manuscript.

LIST OF ABBREVIATIONS

ANOVA	=	Analysis of Variance
ARRIVE	=	Animal Research: Reporting of *In Vivo* Experiments
AF	=	Atretic Follicle(s)
Akt	=	Protein Kinase B
BW	=	Body Weight
Cd	=	Cadmium
$CdCl_2$	=	Cadmium Chloride
CL	=	Corpus Luteum/Corpora Lutea
CMC	=	Carboxymethyl Cellulose
Cm	=	Curcumin
H&E	=	Hematoxylin and Eosin
LH	=	Luteinizing Hormone
FSH	=	Follicle-Stimulating Hormone
NPs	=	Nanoparticles
Nrf2	=	Nuclear Factor Erythroid 2–Related Factor 2
OECD	=	Organisation for Economic Co-operation and Development
PCL	=	Polycaprolactone
PI3K	=	Phosphoinositide 3-Kinase
PLGA	=	Poly(lactic-co-glycolic acid)
PVA	=	Polyvinyl Alcohol

ROS = Reactive Oxygen Species

SD = Standard Deviation

SF = Secondary Follicle

PF = Primary Follicle

UV = Ultraviolet

ETHICS APPROVAL AND CONSENT TO PARTICIPATE

This study is approved by the ethics and policy committee of the College of Veterinary Medicine, Al-Qadisiyah University, Iraq (No. 1180).

HUMAN AND ANIMAL RIGHTS

All experimental protocols were approved by the Institutional Animal Care and Use Committee (IACUC). This study adhered to internationally accepted standards for animal research, following the 3Rs principle. The ARRIVE guidelines were employed for reporting experiments involving live animals, promoting ethical research practices.

CONSENT FOR PUBLICATION

Not applicable.

AVAILABILITY OF DATA AND MATERIALS

The data supporting the findings of the article is available in the Zenodo Repository [https://doi.org/10.5281/zenodo.21779164 and https://doi.org/10.5281/zenodo.21779163].

FUNDING

None.

CONFLICT OF INTEREST

The authors declare no conflict of interest, financial or otherwise.

ACKNOWLEDGEMENTS

The authors present their acknowledgments to the deanery of the College of Veterinary Medicine, University of Al-Qadisiyah, Iraq.

REFERENCES

[1] O. Faroon, A. Ashizawa, S. Wright, P. Tucker, K. Jenkins, L. Ingerman, and C. Rudisill, *Toxicological Profile for Cadmium*, Agency for Toxic Substances and Disease Registry (US): Atlanta (GA), 2012. [PMID: 24049863]

[2] G. Genchi, M.S. Sinicropi, G. Lauria, A. Carocci, and A. Catalano, "The effects of cadmium toxicity", *Int. J. Environ. Res. Public Health*, vol. 17, no. 11, p. 3782, 2020. [http://dx.doi.org/10.3390/ijerph17113782] [PMID: 32466586]

[3] A.Z. Pollack, S. Ranasinghe, L.A. Sjaarda, and S.L. Mumford, "Cadmium and reproductive health in women: A systematic review of the epidemiologic evidence", *Curr. Environ. Health Rep.*, vol. 1, no. 2, pp. 172-184, 2014. [http://dx.doi.org/10.1007/s40572-014-0013-0] [PMID: 27453808]

[4] Z. Qu, L. Liu, X. Wu, P. Guo, Z. Yu, P. Wang, Y. Song, S. Zheng, and N. Liu, "Cadmium-induced reproductive toxicity combined with a correlation to the oogenesis process and competing endogenous RNA networks based on a Caenorhabditis elegans model", *Ecotoxicol. Environ. Saf.*, vol. 268, p. 115687, 2023. [http://dx.doi.org/10.1016/j.ecoenv.2023.115687] [PMID: 37976926]

[5] S. Saedi, M.R. Namavar, M.R.J. Shirazi, F.M. Rezazadeh, and K. Tsutsui, "Exposure to cadmium alters the population of glial cell types and disrupts the regulatory mechanisms of the HPG axis in prepubertal female rats", *Neurotox. Res.*, vol. 40, no. 4, pp. 1029-1042, 2022. [http://dx.doi.org/10.1007/s12640-022-00516-4] [PMID: 35639248]

[6] J.J.V. Branca, C. Fiorillo, D. Carrino, F. Paternostro, N. Taddei, M. Gulisano, A. Pacini, and M. Becatti, "Cadmium-induced oxidative stress: Focus on the central nervous system", *Antioxidants*, vol. 9, no. 6, pp. 492-492, 2020. [http://dx.doi.org/10.3390/antiox9060492]

[7] C. Xiao, and D. Lai, "Impact of oxidative stress induced by heavy metals on ovarian function", *J. Appl. Toxicol.*, vol. 45, no. 1, pp. 107-116, 2025. [http://dx.doi.org/10.1002/jat.4664] [PMID: 38938153]

[8] M. Nasiadek, M. Danilewicz, M. Klimczak, J. Stragierowicz, and A. Kilanowicz, "Subchronic exposure to cadmium causes persistent changes in the reproductive system in female wistar rats", *Oxid. Med. Cell. Longev.*, vol. 2019, pp. 1-17, 2019. [http://dx.doi.org/10.1155/2019/6490820] [PMID: 31949881]

[9] P. Massányi, M. Massányi, R. Madeddu, R. Stawarz, and N. Lukáč, "Effects of cadmium, lead, and mercury on the structure and function of reproductive organs", *Toxics*, vol. 8, no. 4, p. 94, 2020. [http://dx.doi.org/10.3390/toxics8040094] [PMID: 33137881]

[10] Y. Santiago-Andres, E. Hernández Álvarez, D. Ochoa Gutierrez, O. Morton Bermea, and T. Fiordelisio, "In vivo effects of cadmium on signaling and secretion of pituitary gonadotrophs in male mice are time-dependent", *J. Endocrinol.*, vol. 267, no. 1, p. e250161, 2025. [http://dx.doi.org/10.1530/JOE-25-0161] [PMID: 40965112]

[11] K.S. Vinanthi Rajalakshmi, W-C. Liu, B. Balamuralikrishnan, A. Meyyazhagan, G. Sattanathan, M. Pappuswamy, K.S. Joseph, K.A. Paari, and J-W. Lee, "Cadmium as an endocrine disruptor that hinders the reproductive and developmental pathways in freshwater fish: A review", *Fishes*, vol. 8, no. 12, p. 589, 2023. [http://dx.doi.org/10.3390/fishes8120589]

[12] S. Hewlings, and D. Kalman, "Curcumin: A review of its effects on human health", *Foods*, vol. 6, no. 10, p. 92, 2017. [http://dx.doi.org/10.3390/foods6100092] [PMID: 29065496]

[13] A.B. Kunnumakkara, D. Bordoloi, G. Padmavathi, J. Monisha, N.K. Roy, S. Prasad, and B.B. Aggarwal, "Curcumin, the golden nutraceutical: Multitargeting for multiple chronic diseases", *Br. J. Pharmacol.*, vol. 174, no. 11, pp. 1325-1348, 2017. [http://dx.doi.org/10.1111/bph.13621] [PMID: 27638428]

[14] A.V. Sirotkin, "The Influence of Turmeric and Curcumin on Female Reproductive Processes", *Planta Med.*, vol. 88, no. 12, pp. 1020-1025, 2022. [http://dx.doi.org/10.1055/a-1542-8992] [PMID: 34416765]

[15] D.A.M. Kamal, N. Salamt, A.N.M. Yusuf, M.I.A.M. Kashim, and M.H. Mokhtar, "Potential Health Benefits of Curcumin on Female Reproductive Disorders: A Review", *Nutrients*, vol. 13, no. 9, p. 3126, 2021. [http://dx.doi.org/10.3390/nu13093126] [PMID: 34579002]

[16] Z. Yan, Y. Dai, H. Fu, Y. Zheng, D. Bao, Y. Yin, Q. Chen, X. Nie, Q. Hao, D. Hou, and Y. Cui, "Curcumin exerts a protective effect against premature ovarian failure in mice", *J. Mol. Endocrinol.*, vol. 60, no. 3, pp. 261-271, 2018. [http://dx.doi.org/10.1530/JME-17-0214] [PMID: 29437881]

[17] B. Li, Q. Weng, Z. Liu, M. Shen, J. Zhang, W. Wu, and H. Liu, "Selection of antioxidants against ovarian oxidative stress in mouse model", *J. Biochem. Mol. Toxicol.*, vol. 31, no. 12, p. e21997, 2017. [http://dx.doi.org/10.1002/jbt.21997] [PMID: 29205955]

[18] M.T. El-Saadony, T. Yang, S.A. Korma, M. Sitohy, T.A. Abd El-Mageed, S. Selim, S.K. Al Jaouni, H.M. Salem, Y. Mahmmod, S.M.

Soliman, S.A.A. Mo'men, W.F.A. Mosa, N.A. El-Wafai, H.E. Abou-Aly, B. Sitohy, M.E. Abd El-Hack, K.A. El-Tarabily, and A.M. Saad, "Impacts of turmeric and its principal bioactive curcumin on human health: Pharmaceutical, medicinal, and food applications: A comprehensive review", *Front. Nutr.,* vol. 9, p. 1040259, 2023. [http://dx.doi.org/10.3389/fnut.2022.1040259] [PMID: 36712505]

[19] T.L. Virk, Q. Liu, Y. Yuan, X. Xu, and F. Chen, "Curcumin as Therapeutic Modulator of Impaired Antioxidant Defense System: Implications for Oxidative Stress-Associated Reproductive Dysfunction", *Biology,* vol. 14, no. 7, p. 750, 2025. [http://dx.doi.org/10.3390/biology14070750] [PMID: 40723310]

[20] P. Anand, A.B. Kunnumakkara, R.A. Newman, and B.B. Aggarwal, "Bioavailability of curcumin: Problems and promises", *Mol. Pharm.,* vol. 4, no. 6, pp. 807-818, 2007. [http://dx.doi.org/10.1021/mp700113r] [PMID: 17999464]

[21] P. Ratnatilaka Na Bhuket, A. El-Magboub, I.S. Haworth, and P. Rojsitthisak, "Enhancement of Curcumin Bioavailability Via the Prodrug Approach: Challenges and Prospects", *Eur. J. Drug Metab. Pharmacokinet.,* vol. 42, no. 3, pp. 341-353, 2017. [http://dx.doi.org/10.1007/s13318-016-0377-7] [PMID: 27683187]

[22] A. Karthikeyan, N. Senthil, and T. Min, "Nanocurcumin: A promising candidate for therapeutic applications", *Front. Pharmacol.,* vol. 11, p. 487, 2020. [http://dx.doi.org/10.3389/fphar.2020.00487] [PMID: 32425772]

[23] A.K. Rashwan, N. Karim, Y. Xu, N.A.N. Hanafy, B. Li, A.H.E. Mehanni, E.M. Taha, and W. Chen, "An updated and comprehensive review on the potential health effects of curcumin-encapsulated micro/nanoparticles", *Crit. Rev. Food Sci. Nutr.,* vol. 63, no. 29, pp. 9731-9751, 2023. [http://dx.doi.org/10.1080/10408398.2022.2070906] [PMID: 35522080]

[24] Y. Fu, Y. Ge, S. Yi, Q. Peng, H. Jiang, and J. Zhou, "Smart nanoparticle delivery systems for curcumin: A targeted strategy to enhance anticancer efficacy and bioavailability", *J. Mater. Sci. Mater. Med.,* vol. 37, no. 1, p. 38, 2026. [http://dx.doi.org/10.1007/s10856-026-07012-7] [PMID: 41661421]

[25] X. Liu, M. Qi, X. Li, J. Wang, and M. Wang, "Curcumin: A natural organic component that plays a multi-faceted role in ovarian cancer", *J. Ovarian Res.,* vol. 16, no. 1, p. 47, 2023. [http://dx.doi.org/10.1186/s13048-023-01120-6] [PMID: 36859398]

[26] E. Smirnova, M. Moniruzzaman, S. Chin, A. Sureshbabu, A. Karthikeyan, K. Do, and T. Min, "A Review of the Role of Curcumin in Metal Induced Toxicity", *Antioxidants,* vol. 12, no. 2, p. 243, 2023. [http://dx.doi.org/10.3390/antiox12020243] [PMID: 36829803]

[27] H.Y. Wu, H.T. Yu, B. Kang, Y.Y. Xuan, H.Q. Zhang, and X.S. Li, "Curcumin nanoparticles and the therapeutic potential of curcumin for musculoskeletal disorders", *Eur. Rev. Med. Pharmacol. Sci.,* vol. 27, no. 20, pp. 9680-9702, 2023. [http://dx.doi.org/10.26355/eurrev_202310_34139] [PMID: 37916332]

[28] H. Hendarto, S.A. Hutama, R.Y. Primariawan, F.F. Alkaff, B.S. Utomo, W. Widjiati, and N. Suzuki, "Nano-curcumin potentially ameliorates hormonal function and follicular counts following the vitrification and transplantation of rat ovarian tissue", *Sci. Rep.,* vol. 15, no. 1, p. 34588, 2025. [http://dx.doi.org/10.1038/s41598-025-18081-z] [PMID: 41044203]

[29] S. Alaee, Z. Khodabandeh, M. Dara, E. Hosseini, and M. Sharma, "Curcumin mitigates acrylamide-induced ovarian antioxidant disruption and apoptosis in female Balb/c mice: A comprehensive study on gene and protein expressions", *Food Sci. Nutr.,* vol. 12, no. 6, pp. 4160-4172, 2024. [http://dx.doi.org/10.1002/fsn3.4076] [PMID: 38873462]

[30] W.J. Darby, "The American Institute of Nutrition", *Fed. Proc.,* vol. 46, no. 2, pp. 235-240, 1987. [PMID: 3542585]

[31] T. Pulingam, P. Foroozandeh, J.A. Chuah, and K. Sudesh, "Exploring Various Techniques for the Chemical and Biological Synthesis of Polymeric Nanoparticles", *Nanomaterials,* vol. 12, no. 3, p. 576, 2022. [http://dx.doi.org/10.3390/nano12030576] [PMID: 35159921]

[32] A.N. González Morales, L.J. López-Giraldo, E. Sogamoso González, and Y. Moscote Chinchilla, "Evaluation of the Efficiency of Encapsulation and Bioaccessibility of Polyphenol Microcapsules from Cocoa Pod Husks Using Different Techniques and Encapsulating Agents", *Processes,* vol. 13, no. 10, p. 3094, 2025. [http://dx.doi.org/10.3390/pr13103094]

[33] K. Toyoda, M. Shibutani, T. Tamura, T. Koujitani, C. Uneyama, and M. Hirose, "Repeated dose (28 days) oral toxicity study of flutamide in rats, based on the draft protocol for the 'Enhanced OECD Test Guideline 407' for screening for endocrine-disrupting chemicals", *Arch. Toxicol.,* vol. 74, no. 3, pp. 127-132, 2000. [http://dx.doi.org/10.1007/s002040050664] [PMID: 10876997]

[34] F.M. El-Demerdash, M.I. Yousef, F.S. Kedwany, and H.H. Baghdadi, "Cadmium-induced changes in lipid peroxidation, blood hematology, biochemical parameters and semen quality of male rats: Protective role of vitamin E and β-carotene", *Food Chem. Toxicol.,* vol. 42, no. 10, pp. 1563-1571, 2004. [http://dx.doi.org/10.1016/j.fct.2004.05.001] [PMID: 15304303]

[35] M. Tarlan, S. Moradi, N. Heidarizade, O. Tavallaei, S. Khazayel, M.H. Farzaei, and J. Echeverría, "The protective role of curcumin in mitigating drug-induced toxicity in male reproductive system", *Front. Pharmacol.,* vol. 16, p. 1620732, 2025. [http://dx.doi.org/10.3389/fphar.2025.1620732] [PMID: 40792206]

[36] Z. Hassan, and G. Khan, "Histological Methods", In: *Molecular Techniques for Studying Viruses.,* Springer: Singapore, 2024. [http://dx.doi.org/10.1007/978-981-99-8097-0_9]

[37] G.W. Snedecor, and W.G. Cochran, *Statistical Methods.,* 8th ed Iowa State University Press: Ames, 1989.

[38] A. Goutam Mukherjee, U. Ramesh Wanjari, K. Renu, B. Vellingiri, and A. Valsala Gopalakrishnan, "Heavy metal and metalloid - induced reproductive toxicity", *Environ. Toxicol. Pharmacol.,* vol. 92, p. 103859, 2022. [http://dx.doi.org/10.1016/j.etap.2022.103859] [PMID: 35358731]

[39] S.C. Das, and H.A. Al-Naemi, "Cadmium toxicity: Oxidative stress, inflammation and tissue injury", *Occup. Dis. Environ. Med.,* vol. 7, no. 4, pp. 144-163, 2019. [http://dx.doi.org/10.4236/odem.2019.74012]

[40] V.U. Nna, U.Z. Usman, E.O. Ofutet, and D.U. Owu, "Quercetin exerts preventive, ameliorative and prophylactic effects on cadmium chloride - induced oxidative stress in the uterus and ovaries of female Wistar rats", *Food Chem. Toxicol.,* vol. 102, pp. 143-155, 2017. [http://dx.doi.org/10.1016/j.fct.2017.02.010] [PMID: 28229914]

[41] S.S. Ruslee, S.S.M. Zaid, I.H. Bakrin, Y.M. Goh, and N.M. Mustapha, "Protective effect of Tualang honey against cadmium-induced morphological abnormalities and oxidative stress in the ovary of rats", *BMC Complement. Med. Ther.,* vol. 20, no. 1, p. 160, 2020. [http://dx.doi.org/10.1186/s12906-020-02960-1] [PMID: 32471398]

[42] A. Quddus, N. Yimer, F.F.A. Jesse, M.A. Basit, M. Amir, and M.S. Islam, "Edible bird's nest protects histomorphology of rat's uterus against cadmium (Cd) toxicity through a reduction of Cd deposition and enhanced antioxidant activity", *Saudi J. Biol. Sci.,* vol. 28, no. 12, pp. 7068-7076, 2021. [http://dx.doi.org/10.1016/j.sjbs.2021.08.012] [PMID: 34867008]

[43] M.R. Islam, A. Rauf, S. Akter, H. Akter, M.I.K. Al-Imran, M.N.H. Fakir, G.K. Thufa, M.T. Islam, H.A. Hemeg, W.A. Abdulmonem, A.S.M. Aljohani, and M. Iriti, "Neuroprotective Potential of Curcumin in Neurodegenerative Diseases: Clinical Insights Into Cellular and Molecular Signaling Pathways", *J. Biochem. Mol. Toxicol.,* vol. 39, no. 8, p. e70369, 2025. [http://dx.doi.org/10.1002/jbt.70369] [PMID: 40678834]

[44] A. Amaroli, I. Panfoli, M. Bozzo, S. Ferrando, S. Candiani, and S. Ravera, "The Bright Side of Curcumin: A Narrative Review of Its Therapeutic Potential in Cancer Management", *Cancers,* vol. 16, no. 14, p. 2580, 2024.

[http://dx.doi.org/10.3390/cancers16142580] [PMID: 39061221]

[45] J.H. Park, B.M. Lee, and H.S. Kim, "Potential protective roles of curcumin against cadmium-induced toxicity and oxidative stress", *J. Toxicol. Environ. Health B Crit. Rev.,* vol. 24, no. 3, pp. 95-118, 2021. [http://dx.doi.org/10.1080/10937404.2020.1860842] [PMID: 33357071]

[46] H.M. Abdel-Ghany, D.M. El-Sisy, and M.E.S. Salem, "A comparative study of effects of curcumin and its nanoparticles on the growth, immunity and heat stress resistance of Nile tilapia (Oreochromis niloticus)", *Sci. Rep.,* vol. 13, no. 1, p. 2523, 2023. [http://dx.doi.org/10.1038/s41598-023-29343-z] [PMID: 36781934]

[47] Y. Lv, R.C. Cao, H.B. Liu, X.W. Su, G. Lu, J.L. Ma, and W.Y. Chan, "Single-Oocyte Gene Expression Suggests That Curcumin Can Protect the Ovarian Reserve by Regulating the PTEN-AKT-FOXO3a Pathway", *Int. J. Mol. Sci.,* vol. 22, no. 12, p. 6570, 2021. [http://dx.doi.org/10.3390/ijms22126570] [PMID: 34207376]

[48] H. Duan, S. Yang, S. Yang, J. Zeng, Z. Yan, L. Zhang, X. Ma, W. Dong, Y. Zhang, X. Zhao, J. Hu, and L. Xiao, "The mechanism of curcumin to protect mouse ovaries from oxidative damage by regulating AMPK/mTOR mediated autophagy", *Phytomedicine,* vol. 128, p. 155468, 2024. [http://dx.doi.org/10.1016/j.phymed.2024.155468] [PMID: 38471315]